

Magnetic activity, high-energy radiation and variability

From young solar analogs to low-mass objects

Conference Paper

Author(s):

Güdel, Manuel

Publication date:

2010

Permanent link:

<https://doi.org/10.3929/ethz-b-000157547>

Rights / license:

[In Copyright - Non-Commercial Use Permitted](#)

Originally published in:

IAU Symposium 264, <https://doi.org/10.1017/S174392130999295X>

Session VII

Effects of magnetic activity on planet formation and evolution

Chair: S. Hasan

Magnetic activity, high-energy radiation and variability: from young solar analogs to low-mass objects

Manuel Güdel

Institute of Astronomy, ETH Zurich
8093 Zurich, Switzerland
email: guedel@astro.phys.ethz.ch

Abstract. Magnetic activity on cool stars expresses itself in a bewildering variety of radiative and particle output originating from magnetic regions between the photosphere and the corona. Given its origin in evolving magnetic fields, most of this output is variable in time. Radiation in the ultraviolet, the extreme ultraviolet, and the X-ray ranges are important for heating and ionizing upper planetary atmospheres and thus driving atmospheric evaporation. Additionally, stellar winds interact with the upper atmospheres and may lead to further erosion. The stellar high-energy output is therefore a prime factor in determining habitability of planets. We summarize our knowledge of magnetic activity in young solar analogs and lower-mass stars and show how the stellar output changes on evolutionary timescales.

Keywords. Sun: evolution, stars: activity, stars: evolution, stars: flare, stars: rotation, stars: magnetic fields, stars: winds, astrobiology

1. Introduction

The present-day Sun is a G2 V star with a surface effective temperature of approximately 5780 K. Stellar evolution theory indicates, however, that the Sun has shifted in spectral type by several subclasses, becoming hotter by a few hundred degrees and becoming more luminous; the bolometric luminosity of the Sun in its zero-age main-sequence [ZAMS] phase amounted to only about 70% of the present-day output (Sackmann & Boothroyd 2003). The lower luminosity poses serious problems with regard to habitability of the young Earth and Mars. While geological records indicate a warmer climate and the presence of liquid water on both planets at ages younger than 1 Gyr, both should have been in deep freeze with sub-zero temperatures. Although greenhouse gases could have made up for the deficit in the case of the young Earth, a higher-pressure CO₂ rich atmosphere on Mars would still not have retained enough energy (Kasting *et al.* 1993; Sackmann & Boothroyd 2003). One potential solution to this problem will be mentioned in Sect. 5 below.

However, the Sun's luminosity changed much more dramatically at shorter wavelengths in the course of its evolution. Direct and indirect evidence points to a much higher level of magnetic activity in particular in its pre-main sequence (PMS) phase, the subsequent epoch of its settling on the main sequence (MS), and the first few 100 Myr of its life on the MS. Direct evidence includes meteoritic traces and isotopic anomalies that require much higher proton fluxes at early epochs at least partly from *within* the solar system (e.g., Caffee *et al.* 1987); indirect evidence comes from systematic comparisons of the contemporary Sun with solar analogs of younger age. Atmospheres of solar system planets offer further clues to strongly elevated activity levels, among them the evidence for a

warmer early climate on Mars but also the extremely arid atmosphere of Venus – a sister planet of the water-rich Earth.

We discuss three topics that are of some importance for our understanding of the young solar system and the evolution of planetary atmospheres. We first discuss the evolution of rotation and activity of solar-like stars and address their elusive ionized winds; we then summarize knowledge of the long-term evolution of the radiative output of the Sun and lower-mass stars; and third, we address the importance of flares in stellar activity. The last section discusses the importance of stellar high-energy output in shaping young planetary environments.

2. The rotation and mass-loss history of the Sun

Stellar magnetic winds are a crucial consequence of “stellar activity” but their detection in solar analogs is very difficult. The best – albeit indirect – proof of the presence of magnetized winds is the spin-down of convective stars on the main sequence as such a wind carries away angular momentum from the star.

Owing to its coupling to large-scale solar magnetic fields, the wind carries away angular momentum, leading to a steady decline of the solar rotation rate. The fractional change in the rotation rate, Ω , is,

$$\frac{\dot{\Omega}}{\Omega} \propto \frac{\dot{M}}{M} \left(\frac{R_A}{R_\odot} \right)^m \quad (2.1)$$

where M is the stellar mass, R_A is the Alfvén radius, and m has a value between 0 and 1 depending on the magnetic field geometry (e.g., Mestel 1984). The surface magnetic field strength itself is coupled to the rotation rate via an internal dynamo and is expected to scale as $B_0 \propto \Omega^p$ with p being 1 or 2 (e.g., Mestel 1984). It has further been suggested that the wind mass loss rate itself scales with magnetic activity (see below); in other words, activity and rotation are coupled by a feedback loop (slower rotation \rightarrow decreasing magnetic activity \rightarrow smaller mass loss rate \rightarrow less magnetic braking) that not only leads to a steadily declining rotation rate during the Sun’s MS life but causes the rotation rate to converge toward a unique age-dependent value for a given stellar mass. This picture has found basic support from the observation of declining magnetic activity with increasing stellar age and rotation periods, as inferred from many open-cluster studies (e.g., Soderblom *et al.* 1993). This evolutionary scheme of rotation and magnetic activity overall holds for all late-type stars but the activity decay is considerably slower toward lower-mass stars (West *et al.* 2008). For solar analogs one finds,

$$\Omega \propto t_6^{-0.6 \pm 0.1} \text{ [d]} \quad (2.2)$$

(Ayres 1997). The rotation period thus decays by typically a factor of about 20 from ZAMS age to the end of the MS life.

Ionized winds have not yet been “directly” detected from any late-type main-sequence star other than the Sun. A potential direct detection method is provided by the measurement of thermal radio emission from the winds. Drake *et al.* (1993) obtained a radio upper limit to the wind mass loss of $\dot{M} < 1.7 \times 10^{-11} M_\odot \text{ yr}^{-1}$ for the *evolved* subgiant Procyon (albeit based on indirect arguments), while Lim *et al.* (1996) found an upper limit of $\dot{M} < 7 \times 10^{-12} M_\odot \text{ yr}^{-1}$ for the nearby, relatively old M dwarf Proxima Centauri. Although the rising spectra suggest high fluxes at millimeter wavelengths, the limited sensitivity available in that domain has not yielded definitive detections; tentative measurements (Doyle & Mathioudakis 1991; Mullan *et al.* 1992) suggested extremely high \dot{M} revisited by Lim & White (1996), Lim *et al.* (1996) and van den Oord *et al.* (1997) who

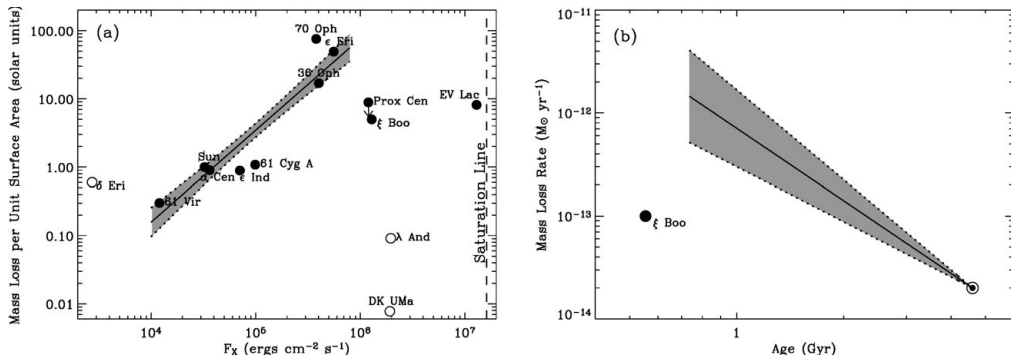


Figure 1. Left (a): Mass-loss rates per unit surface area vs. stellar X-ray surface fluxes inferred indirectly from Ly α analysis. MS stars are shown by filled circles. The trend for inactive stars (shaded area) is not followed by more active stars. – Right (b): Inferred mass-loss history of the Sun. The trend shown for inactive stars (shaded area) breaks down for the youngest, most active stars (from Wood *et al.* 2005), reproduced by permission of AAS.

argued against a wind interpretation. Interesting upper limits ($\dot{M} < 10^{-10} - 10^{-9} M_\odot \text{ yr}^{-1}$) were also obtained for A and F-type stars, indicating that their mass loss is not critically altering their evolution (Brown *et al.* 1990). Gaidos *et al.* (2000) specifically focused on *young solar analogs*. The most stringent upper limits were set for the G stars π^1 UMa, κ^1 Cen and β Com, namely $\dot{M} < 4 - 5 \times 10^{-11} M_\odot \text{ yr}^{-1}$ (3σ), constraining the total mass loss in the solar history after arrival on the ZAMS to $\approx 6\%$ of M_\odot (Gaidos *et al.* 2000).

Another method to detect ionized winds directly is the search for charge exchange signatures due to interactions between wind ions and neutrals from the interstellar medium within the “astrospheres” (see below) of nearby stars. This method has provided a tight upper limit of $\dot{M} < 3 \times 10^{-13} M_\odot \text{ yr}^{-1}$ for Proxima Centauri (Wargelin *et al.* 2002).

The most promising (indirect) approach to date makes use of Ly α absorption in so-called “astrospheres”. When solar/stellar winds collide with the interstellar medium, they form, with increasing distance from the star, a termination shock (where the wind is shocked to subsonic speeds), a heliosphere (separating the plasma flows from the star and the ISM), and the bow shock (where the ISM is shocked to subsonic speeds). The heliosphere is permeated by interstellar H I with $T \approx (2 - 4) \times 10^4$ K (Wood *et al.* 2002). Much of this gas is piled up between the heliosphere and the bow shock, forming the so-called “hydrogen wall” that can be detected as an absorption signature in the Ly α line. The excess absorption from the Sun’s own hydrogen wall is, due to the deceleration of the ISM relative to the star, redshifted, while that of other astrospheres is blueshifted.

The measurable absorption depths in Ly α are compared with results from hydrodynamic model calculations (Wood *et al.* 2002, Wood *et al.* 2005). The amount of astrospheric absorption should scale with the wind ram pressure, $P_w \propto \dot{M}_w V_w$, where V_w is the (unknown) wind velocity (Wood & Linsky 1998). The latter is usually assumed to be the same as the solar wind speed, i.e., a few 100 km s^{-1} . Consequently, \dot{M}_w can be derived. A systematic study of a sample of nearby stars at different activity levels shows that \dot{M}_w per unit stellar surface correlates with the stellar X-ray surface flux,

$$\dot{M}_w \propto F_X^{1.34 \pm 0.18} \quad (2.3)$$

(an equivalent relation therefore holds between \dot{M}_w and L_X); using the activity-age relation (see below), one finds

$$\dot{M}_w \propto t^{-2.33 \pm 0.55} \quad (2.4)$$

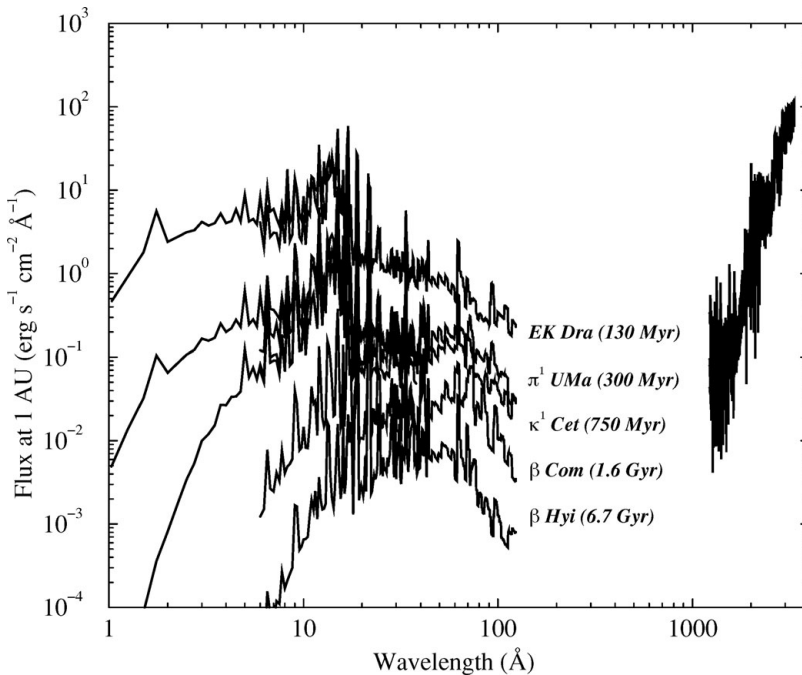


Figure 2. UV, EUV, and X-ray irradiances at 1 AU from solar analogs with different ages (from Guinan & Ribas 2002, reprinted with permission of ASP).

(Wood *et al.* 2005). If stellar-wind mass loss could be measured directly, it would be a genuine magnetic activity indicator, because mass-loss is higher in young, magnetically active stars than in evolved stars.

3. The radiative history of magnetically active stars

As stars arrive on the MS, their initial rotation period may differ largely as a consequence of different star-disk coupling and disk-dispersal histories. Nevertheless, magnetic activity, best expressed by the stellar X-ray luminosity (L_X), remains narrowly confined at predictable levels during this phase. This is because most stars rotate rapidly enough to keep them in the empirical saturation regime where L_X is controlled essentially by L_{bol} , $L_X \approx 10^{-3} L_{\text{bol}}$ (e.g., Randich *et al.* 2000), rather than by rotation.

Once stars have spun down sufficiently, they enter the regime where $L_X \propto P^{-2}$ (Pizzolato *et al.* 2003), i.e., $L_X \propto t^{-1.2}$ where t is the stellar age. This phase starts a few 100 Myr after arrival on the ZAMS for a solar-mass star, but the saturation phase takes much longer for M dwarfs (1 Gyr and longer, see West *et al.* 2008). This very slow evolution of magnetic activity in M dwarfs is potentially important for planets in their habitable zones. The high L_X (relative to L_{bol} defining the habitable zone) affects planetary atmospheres (and potentially the presence of water) for a much longer time than for a more massive star (e.g., Scalo *et al.* 2007).

Similar decay laws hold for other short-wavelength radiation. Ultraviolet excess emission from late-type stars originates in magnetic chromospheric and transition-zone regions that have been heated to temperatures of order $10^4 - 10^5$ K. Ribas *et al.* (2005) studied the ultraviolet decay for the “Sun in Time” sample. The bulk of the UV flux in the region shortward of 1700 \AA is in emission lines while the continuum is negligible. Emission lines include those of O I $\lambda 1304$, C II $\lambda 1335$, Si IV $\lambda 1400$, C IV $\lambda 1550$, He II $\lambda 1640$, and C I $\lambda 1657$.

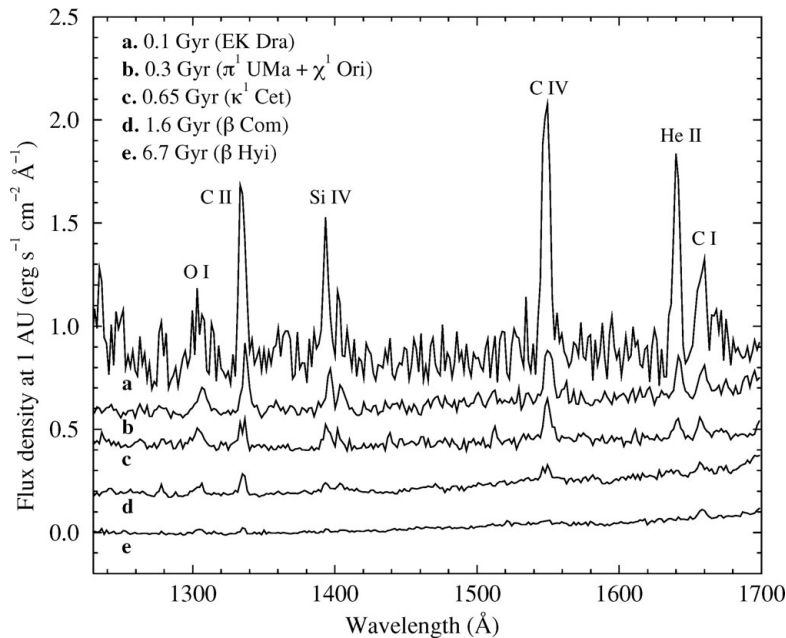


Figure 3. Extracts of UV spectra of solar analogs with different ages. All spectral fluxes have been transformed to irradiances at 1 AU from the star. The spectra have been shifted along the ordinate, by multiples of $0.2 \text{ erg s}^{-1} \text{ cm}^{-2} \text{ \AA}^{-1}$ (from Ribas *et al.* 2005, reproduced by permission of AAS).

Although the corresponding line fluxes decay in time, the decay law is shallower than for X-rays. A comparison of line spectra is shown in Fig. 3.

This study was also extended into the far-UV (FUV) region, finding that the power-law decay is steeper than for chromospheric lines, but shallower than for coronal fluxes or luminosities. The decay of EUV fluxes closely follows the decay of X-ray fluxes as they are both dominated by coronal lines.

These elements can be put together to construct a comprehensive model of the spectral evolution of the “Sun in Time” in the wavelength band that is relevant for ionization of and chemical reactions in planetary atmospheres, i.e. the 1–1700 Å FUV/EUV/X-ray (“XUV”) range, as presented by Ribas *et al.* (2005). These authors computed band-integrated irradiances for the spectral ranges of 1–20 Å (X-rays), 20–100 Å (soft X-rays and EUV), 100–360 Å (EUV), and 920–1180 Å (FUV). For the wavelength range of 1180–1700 Å, only line fluxes are relevant for the study of magnetically induced emission because the continuum is dominated by photospheric contributions.

All integrated irradiances correlate tightly with the stellar rotation period or age, suggesting a rapid decay of activity at all atmospheric levels in concert. The relations are well represented by power laws, as illustrated in Figure 4. From band-integrated luminosities and individual lines (see Telleschi *et al.* 2005 for X-ray lines) the following decay laws are found for chromospheric, transition region UV, transition region FUV, EUV (including the softest X-rays at 20–100 Å), and soft X-rays (1–20 Å), where we also use the rotation law in Eq. (2.2):

$$L_{\text{ch}} \propto P^{-1.25 \pm 0.15} \propto t^{-0.75 \pm 0.1} \quad (3.1)$$

$$L_{\text{UV}} \propto P^{-1.60 \pm 0.15} \propto t^{-1.0 \pm 0.1} \quad (3.2)$$

$$L_{\text{FUV}} \propto P^{-1.40} \propto t^{-0.85} \quad (3.3)$$

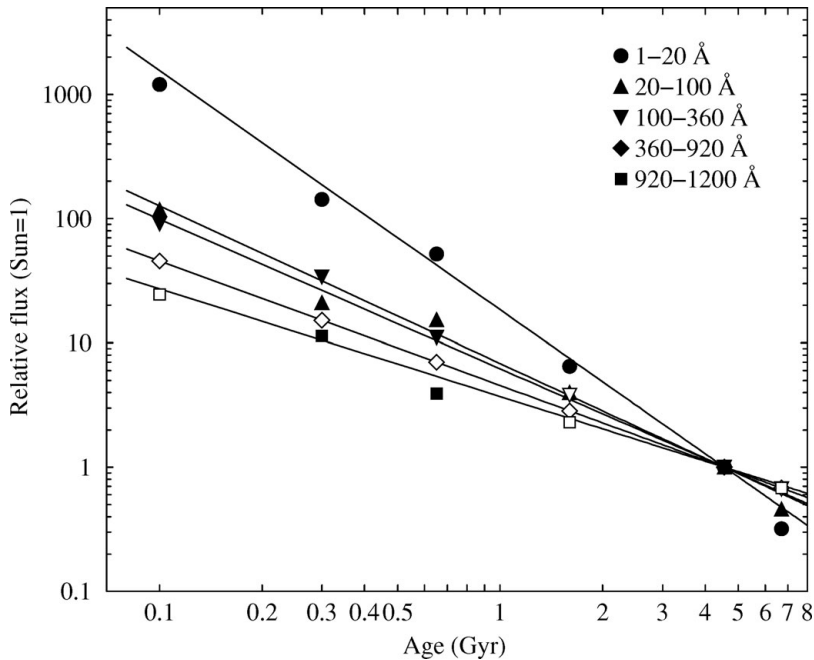


Figure 4. Power-law decays in time for various spectral ranges, normalized to the present-day solar flux. Note that the hardest emission decays fastest (from Ribas *et al.* 2005, reproduced by permission of AAS).

$$L_{\text{EUV}} \propto P^{-2.0} \quad \propto t^{-1.2} \quad (3.4)$$

$$L_{\text{X}} \propto P^{-3.2} \quad \propto t^{-1.9} \quad (3.5)$$

4. Flares and the highest energy photons

Coronal magnetic flares heat plasma explosively to $\gtrsim 10$ MK on time scales of minutes, and radiate at elevated levels for up to many hours. In a standard model of solar flares, a magnetic reconnection process taking place high in the corona accelerates electrons to (at least) hundreds of keV. Electron beams impact in the lower atmosphere where they deposit their energy in the chromospheric gas. Part of the energy is radiated in hard X-rays (HXR) and gamma rays. As a consequence of the heating, the high-pressure gas evaporates into the magnetic loops of the corona, where it loses its energy by radiation and conduction. This is the main phase of the soft X-ray flare. Some flares, in particular the most energetic examples, are accompanied by ejection of plasma clouds, the “Coronal Mass Ejections” (CMEs) that join the stellar wind at high velocities.

Most of these flare signatures can be observed on stars, the most crucial exception being the non-thermal HXR component for which sensitive detectors are not yet available. Osten *et al.* (2007) reported a case of a giant flare on an RS CVn binary detecting photons up to 100 keV with a spectrum compatible with a power-law although a thermal bremsstrahlung continuum from a superhot (> 100 MK) plasma component cannot be excluded. The HXR radiation was unusual in that it was recorded throughout the gradual phase of the flare. If interpreted as a power-law, the spectrum indicates an energy power-law index for the colliding electrons of $\delta \approx 3$, a value very similar to those inferred from solar HXR flares.

Flares may solve a long-standing riddle in solar physics, namely the problem of coronal heating. Many flares are too small to be recognized individually in disk-integrated light curves, but these are the most frequent events and may thus contribute significantly to coronal heating. This assumption is known as the “microflare” or “nanoflare” hypothesis in solar physics (Parker 1988). In the solar case, hard-X-ray studies have shown that flares are distributed in energy according to a power law,

$$\frac{dN}{dE} = kE^{-\alpha} \quad (4.1)$$

where dN is the number of flares per unit time with a total energy in the interval $[E, E + dE]$, and k is a constant. If $\alpha \geq 2$, then the energy integration (for a given time interval, $\int_{E_{\min}}^{E_{\max}} E[dN/dE]dE$) diverges for $E_{\min} \rightarrow 0$, that is, if the power law is extrapolated to small flare energies, a lower cut-off is required for the power-law distribution. On the other hand, any energy release power is possible depending on the value of E_{\min} .

Such distributions apply equally to stars. Studies have used X-rays and extreme ultraviolet radiation to find α mostly in the range of 2–2.5 for G–M dwarfs (Audard *et al.* 2000; Kashyap *et al.* 2002; Güdel *et al.* 2003) and for T Tauri stars (Stelzer *et al.* 2007), supporting the view that moderate flares are the dominant heating source for these active coronae. This observation may indeed be the basis for the correlation between radio and soft X-ray emission in magnetically active stars and flares, the high level of apparently constant emission being the result of a large number of comparatively small flares not individually detected in the light curves (Telleschi *et al.* 2005).

There is further evidence supporting this model. Specifically, the rate of EUV flares above a given threshold scales linearly with the average X-ray luminosity of a late-type star (Audard *et al.* 2000), a relation that was suggested to apply to T Tauri stars as well (Stelzer *et al.* 2007).

The statistical flare model has some implications for the production of HXR and gamma-ray emission as well as energetic particles and CMEs. As seen in the Sun, accelerated particles produce HXR bursts in the impulsive flare phase, with a total HXR energy scaling non-linearly with the soft X-ray energy (Battaglia *et al.* 2005). Combining this scaling with Eq. (4.1) predicts a quasi-steady, average HXR luminosity of a few times $10^{-5} L_X$ (Güdel 2009, see also Caramazza *et al.* 2009). This radiation could contribute to heating and ionization of upper planetary atmospheres, with a larger penetration depth than soft X-rays or EUV photons.

5. High-energy radiation and the stellar environment

The ionized and magnetized solar wind interacts strongly with planetary magnetospheres and atmospheres, inducing such phenomena as aurorae or “ionospheric disturbances”, but at a more fundamental level, wind-planet interactions have played an important role in the formation and evolution of planetary atmospheres and consequently the formation of life on Earth. Interactions between the upper planetary atmosphere/ionosphere and the wind or related electric and magnetic fields lead to continuous atmospheric erosion as ions are carried away. The most crucial processes are related to ion pick-up, sputtering, ionospheric outflow, and also dissociative recombination; the ionizing source for the upper planetary atmosphere is the EUV and X-ray emission from the Sun (for a summary see, e.g., Chassefière & Leblanc 2004, Kulikov *et al.* 2007, and Lundin *et al.* 2007). These processes are thought to have fundamentally altered the atmospheres

of Venus, Earth, and Mars, leading to strong loss of oxygen (Lammer *et al.* 2006) and therefore water (after photodissociation of water vapor in the upper atmosphere) from young Venus and Mars. A strong magnetosphere around the Earth, shielding the lower atmospheric layers, may have been instrumental in retaining much of its water and making it habitable. Nevertheless, the amount of shielding depends on the strength of the wind and its ability to compress the magnetosphere.

Planets such as “hot Jupiters”, but also planets in the close-in “habitable zones” around low-mass M dwarfs, rapidly evolve toward slow, tidally locked rotation, i.e., a rotation period equal to the orbit period of several days. As a consequence, the dynamo-generated magnetic moment will be comparatively small, and the ram pressure of the solar/stellar wind will compresses the magnetosphere sufficiently to expose the upper atmosphere to the solar/stellar wind; this effect is particularly strong if the upper atmosphere is heated and expanded by strong EUV/X-ray flux from a magnetically active central star. Magnetic protection of the atmosphere is thus strongly reduced (Grießmeier *et al.* 2005; Lammer *et al.* 2007). At the same time, the cosmic ray flux above the planetary atmosphere will be enhanced given the weaker and smaller magnetosphere (Grießmeier *et al.* 2005).

Coronal mass ejections (CME), often accompanying large flares, add significantly to atmospheric erosion. An ejection rate of several CMEs per day will essentially act like an enhanced solar wind, which will further compress planetary magnetospheres and erode the upper atmospheres (Khodachenko *et al.* 2007). The combination of enhanced exospheric heating by EUV irradiation with consequent exospheric expansion and a CME “wind” could induce atmospheric losses of up to tens or hundreds of bars for close-in planets. This may again be particularly important for planets in the habitable zones around M dwarfs (Lammer *et al.* 2007).

Increased wind mass loss rates may solve the *Faint Young Sun Paradox* (FYSP) emerging from evidence that the young Earth (and Mars) maintained a mild climate and carried liquid surface water although standard evolutionary models indicate that the zero-age main-sequence (ZAMS) Sun was bolometrically 30% fainter than at present (leading to global freeze-out of water). A higher mass loss rate in the Sun’s early evolution would suggest a higher initial mass, M_i , and therefore higher bolometric luminosity (Whitmire *et al.* 1995; Sackmann *et al.* 2003). M_i is bounded by $1.07M_\odot$ to prevent the young Earth from losing its water reservoir through a moist greenhouse (Sackmann & Boothroyd 2003 and references therein, see Fig. 5). But to allow liquid water on the Martian surface *even in the presence of an extreme CO₂ greenhouse*, $M_i \gtrsim 1.03 - 1.04 M_\odot$ is required, depending on the functional form of the mass-loss history (Sackmann *et al.* 2003; Whitmire *et al.* 1995). This would require $\dot{M}_i \approx 10^{-11} - 10^{-10} M_\odot \text{ yr}^{-1}$ (Sackmann *et al.* 2003), steadily declining to present-day levels according to Eq. (2.1).

The required mass loss rates are in a range that is becoming accessible to radio-astronomical observations. As mentioned in Sect. 2, Gaidos *et al.* (2000) constrained the total mass loss in the solar history to $\approx 6\%$ of M_\odot using upper limits to radio fluxes from young solar analogs and a power-law decay law of the form given in Eq. (2.1), i.e., a wind-decay law following $\dot{M} \propto t^{-1}$.

Mass loss rates derived indirectly using the Ly α method (see Sect. 2) are too small for the above requirement. Following the results from the Wood *et al.* studies, the integrated mass loss during the past 4.5 Gyr history of the Sun would amount to only $0.003M_\odot$. We note, however, that the apparent breakdown of the observed relation for very active (young) stars remains unexplained, and that the Ly α method relies on a rather indirect interpretation that should be confirmed using other approaches.

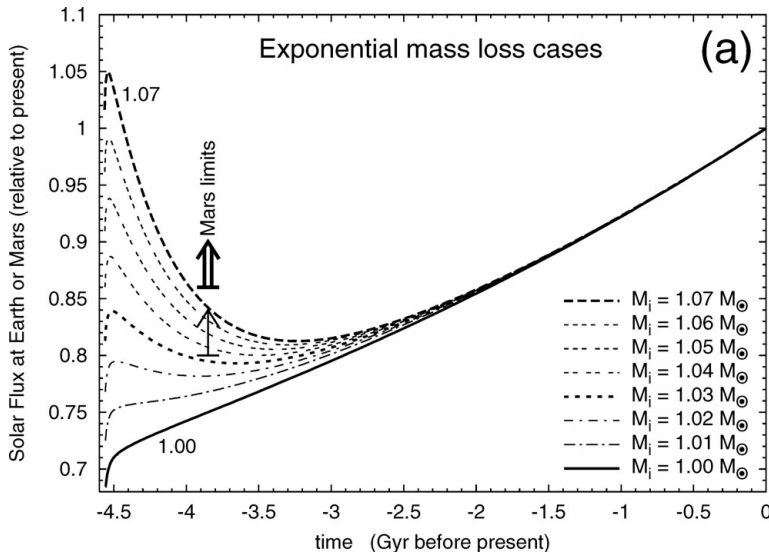


Figure 5. Solar flux in time with respect to present, assuming that the young Sun was subject to increased mass loss. Different curves show calculations for different initial masses, i.e., different mass loss rates that evolve to a mass of $1M_{\odot}$ after 4.6 Gyr. It has been assumed that the mass-loss rate declines exponentially in time. The flux increase at intermediate to high ages corresponds to the evolutionary increase of the Sun for nearly constant mass. The double arrow indicates the lower limit required for the presence of liquid water on early Mars, the thin arrow an (unrealistic) extreme lower limit. Preservation of water on Earth requires the solar flux to remain below 1.1 times the present-day flux (from Sackmann *et al.* 2003, reproduced by permission of AAS).

6. Summary

While the young Sun was bolometrically 30% fainter than the present-day Sun, its magnetic activity has declined continuously as it has been spinning down due to mass loss in a magnetized wind. As a consequence, magnetically induced short-wavelength radiation has decreased by orders of magnitude in particular at the shortest (X-ray) wavelengths. Similar trends apply to lower-mass stars although their magnetic evolution is slower. Young planets were subject to much higher XUV irradiation, inducing enhanced photochemistry, ionization and heating of their upper atmospheres, with serious consequences for the presence of water and habitability. Another key feature of active stars is their ionized wind that has also been suggested to steadily decrease during a star's MS evolution. It further contributes to erosion of planetary atmospheres. On the other hand, a more massive young Sun undergoing much stronger mass loss may have prevented the young Earth and Mars from a deep freeze.

References

- Audard, M., Güdel, M., Drake, J. J., & Kashyap, V. L. 2000, *ApJ*, 541, 396
 Ayres, T. R. 1997, *J. Geophys. Res.*, 102, 1641
 Battaglia, M., Grigis, P. C., & Benz, A. O. 2005, *A&A* 439, 737
 Brown, A., Veale, A., Judge, P., Bookbinder, J. A., & Hubeny, I. 1990, *ApJ*, 361, 220
 Caffee, M. W., Hohenberg, C. M., Swindle, T. D., & Goswami, J. N. 1987, *ApJ*, 313, L31
 Caramazza, M., Drake, J. J., Micela, G., & Flaccomio, E. 2009, *A&A*, 503, 505
 Chassefière, E. & Leblanc, F. 2004, *Planet. Space Sci.*, 52, 1039
 Doyle, J. G. & Mathioudakis, M. 1991, *A&A*, 241, L41

- Drake, S. A., Simon, T., & Brown, A. 1993, *ApJ*, 406, 247
- Gaidos, E. J., Güdel, M., & Blake, G. A. 2000, *Geophys. Res. Lett.*, 27, 501
- Güdel, M. 2009, in *Simbol-X: Focusing on the Hard X-Ray Universe*, AIP Conf. Proc. 1126, 341
- Güdel, M., Audard, M., Kashyap, V. L., Drake, J. J., & Guinan, E. F. 2003, *ApJ*, 582, 423
- Guinan, E. F. & Ribas, I. 2002, in ASP Conf. Ser. 269 Eds. Montesinos, B., Giménez, A., & Guinan, E. F. (San Francisco: ASP), 85
- Grieffmeier, J.-M., Stadelmann, A., Motschmann, U., Belisheva, N. K., Lammer, H., & Biernat, H. K. 2005, *Astrobiology* 5, 587
- Kashyap, V. L., Drake, J. J., Güdel, M., & Audard, M. 2002, *ApJ*, 580, 1118
- Kasting, J. F., Whitmire, D. P., & Reynolds, R. T. 1993, *Icarus*, 101, 108
- Khodachenko, M. L., Ribas, I., Lammer, H., Grieffmeier, J.-M., Leitner, M., *et al.* 2007, *Astrobiology* 7, 167
- Kulikov, Y. N., Lammer, H., Lichtenegger, H. I. M., Penz, T., Breuer, D., *et al.* 2007, *Space Sci. Rev.*, 129, 207
- Lammer, H., Lichtenegger, H. I. M., Biernat, H. K., Erkaev, N. V., Arshukova, I. L., *et al.* 2006, *Planet. Space Sci.*, 54, 1445
- Lammer, H., Lichtenegger, H. I. M., Kulikov, Y. N., Grieffmeier, J.-M., Terada, N., *et al.* 2007, *Astrobiology* 7, 185
- Lim, J. & White, S. M. 1996, *ApJ*, 462, L91
- Lim, J., White, S. M., & Slee, O. B. 1996, *ApJ*, 460, 976
- Lundin, R., Lammer, H., & Ribas, I. 2007, *Space Sci. Rev.*, 129, 245
- Mestel, L. 1984, in *Cool Stars, Stellar Systems, and the Sun: Third Cambridge Workshop*, Eds. Baliunas, S. L., & Hartmann, L. (New York: Springer) 49
- Mullan, D. J., Doyle, J. G., Redman, R. O., & Mathioudakis, M. 1992 *ApJ*, 397, 225
- Osten, R. A., Drake, S., Tueller, J., Cummings, J., Perri, M., *et al.* 2007, *ApJ*, 654, 1052
- Parker, E. N. 1988, *ApJ*, 330, 474
- Pizzolato, N., Maggio, A., Micela, G., Sciortino, S., & Ventura, P. 2003, *A&A*, 397, 147
- Randich, S. 2000, in *Stellar Clusters and Associations: Convection, Rotation, and Dynamos*, eds. R. Pallavicini, G. Micela, & S. Sciortino, (San Francisco: ASP), 401
- Ribas, I., Guinan, E. F., Güdel, M., & Audard, M. 2005, *ApJ*, 622, 680
- Scalo, J., Kaltenecker, L., Segura, A. G., Fridlund, M., Ribas, I., *et al.* 2007, *Astrobiology*, 7, 85
- Sackmann, I.-J. & Boothroyd, A. I. 2003, *ApJ*, 583, 1024
- Soderblom, D. R., Stauffer, J. R., MacGregor, K. B., & Jones, B. F. 1993, *ApJ*, 409, 624
- Stelzer, B., Flaccomio, E., Briggs, K., Micela, G., Scelsi, L., *et al.* 2007, *A&A*, 468, 463
- Telleschi, A., Güdel, M., Briggs, K., Audard, M., Ness, J.-U., & Skinner, S. L. 2005, *ApJ*, 622, 653
- van den Oord, G. H. J. & Doyle, J. G. 1997, *A&A*, 319, 578
- Wargelin, B. J. & Drake, J. J. 2002, *ApJ*, 578, 503
- West, A. A., Hawley, S. L., Bochanski, J. J., Covey, K. R., Reid, I. N., *et al.* 2008, *AJ*, 135, 785
- Whitmire, D. P., Doyle, L. R., Reynolds, R. T., & Matese, J. J. 1995, *J. Geophys. Res.*, 100, 5457
- Wood, B. E. & Linsky, J. L. 1998, *ApJ* 492, 788
- Wood, B. E., Müller, H.-R., Zank, G. P., & Linsky, J. L. 2002, *ApJ*, 574, 412
- Wood, B. E., Müller, H.-R., Zank, G. P., Linsky, J. L., Redfield, S. 2005, *ApJ*, 628, L143